Journal of Molecular Structure 1030 (2012) 157–167

Contents lists available at SciVerse ScienceDirect

Journal of Molecular Structure

journal homepage: www.elsevier.com/locate/molstruc

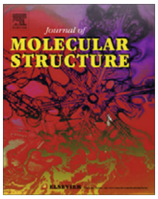

Structural and vibrational studies on (*E*)-2-(2-hydroxy benzyliden amino)-3-phenyl propionic acid using experimental and DFT methods

H. Saleem [a,*], Y. Erdogdu [b], S. Subashchandrabose [a], V. Thanikachalam [c], J. Jayabharathi [c], N. Ramesh Babu [a]

[a] *Dept. of Physics, Annamalai University, Annamalai Nagar, Tamil Nadu 608 002, India*
[b] *Dept. of Physics, Ahi Evran University, 40040 Kirsehir, Turkey*
[c] *Dept. of Chemistry, Annamalai University, Annamalai Nagar, Tamil Nadu 608 002, India*

ARTICLE INFO

Article history:
Received 17 December 2011
Received in revised form 3 April 2012
Accepted 5 April 2012
Available online 12 April 2012

Keywords:
Phenylalanine
Salicylaldehyde
FT-IR
FT-Raman
TED

ABSTRACT

The structural and spectroscopic properties of (*E*)-2-(2-hydroxy benzyliden amino)-3-phenyl propionic acid ((*E*)-2-HBAPPA) has been investigated by using theoretical and experimental methods. Using the computational studies the most stable conformer was identified. Density functional theory (DFT) calculations of 16 (*E*)-2-HBAPPA conformers have been performed to find the optimized structure and the computed vibrational wavenumbers of the most stable one. The FT Raman and FT-IR spectra of (*E*)-2-HBAPPA molecule have been recorded and analyzed. A detailed interpretation of the FT-IR, FT-Raman and harmonic wavenumbers obtained at B3LYP/6-311++G(d,p) level was reported. The vibrational assignments were studied using TED method. Intra-molecular charge transfer between nitrogen and hydroxyl hydrogen ($C{=}N\cdots H{-}O$) has been studied. First order hyperpolarizability (β_0) has been calculated. Electronic excitation of (*E*)-2-HBAPPA was recorded in the visible region and compared with calculated TD-DFT results.

1. Introduction

The *ortho*-hydroxy Schiff bases have received much attention in different areas such as biology, coordination chemistry, technological applications and chemical physics [1–4]. Salicylideneaniline Schiff bases which has long-ranged π-electron delocalization capacity affecting whole molecule during the proton transfer reaction, $O{-}H\cdots N \leftrightarrow H\cdots N$ [5,6]. The easiest intra molecular interaction of this type of compound leads the molecule, used as a potential material for molecular memory, photo switch device and models of biological system [7–9].

The pharmaceutical studies [10–12], revealed great potential in the application of *ortho*-hydroxy acylaromatic Schiff bases as cancer fighters. Schiff bases compound also exhibit a wide range of biological activities such as anti-HIV [13–15] anti-tumor [16], antiviral activity [17] antimicrobial activity [18], and anti-inflammatory activity [19].

The present work mainly deals with detailed structural conformation, experimental FT-IR and FT-Raman spectra, intra-molecular hydrogen bonding, vibrational assignments using total energy distribution (TED) and NLO activity as well as DFT/B3LYP calculations for (*E*)-2-HBAPPA. The vibrational spectral features of (*E*)-2-HBAPPA compound have not been subject of detailed analysis so far. Herein, the investigated results have been reported. The experimental and theoretical results support each other, and the calculations are valuable for providing a reliable insight into the vibrational spectra and molecular properties.

2. Experimental details

2.1. Synthesis

This compound was synthesized by mixing the salicylaldehyde in ethanol and sodium salt of phenylalanine in ethanol–water (50% v/v). The mixture was heated and refluxed on a mantel about 5 h. The reaction mixture was cooled to room temperature and neutralized by 1:1 HCl. The white Schiff base was separated, filtered off, washed thoroughly with deionised water ethanol mixture followed by ether wash. The product obtained was dried over vacuum desiccators. The melting point of the compound is 114 °C (lit 114 °C) [20].

2.2. FT-Raman and FT-IR spectra

The FT-Raman spectrum of (*E*)-2-HBAPPA was recorded using the 1064 nm line of a Nd:YAG laser as excitation wavelength in the region 10–3500 cm^{-1} on a Bruker model IFS 66 V spectrophotometer equipped with an FRA 106 FT-Raman module accessory.

---

* Corresponding author.
E-mail addresses: saleem_h2001@yahoo.com (H. Saleem), yusuferdogdu@gmail.com (Y. Erdogdu), sscbphyscis@gmail.com (S. Subashchandrabose).

0022-2860/$ - see front matter © 2012 Elsevier B.V. All rights reserved.
http://dx.doi.org/10.1016/j.molstruc.2012.04.011

The spectral measurements were carried out at Sree Chitra Tirunal Institute for Medical Sciences and Technology, Poojappura, Thiruvananthapuram, Kerala, India. The FT-IR spectrum of this compound was recorded in the region 400–4000 cm^{-1} on an IFS 66 V spectrophotometer using the KBr pellet technique. The spectrum was recorded at room temperature, with a scanning speed of 10 cm^{-1} per minute and at the spectral resolution of 2.0 cm^{-1} in CISL Laboratory, Annamalai University, and Tamilnadu, India. The UV spectrum was recorded using Perkin Elmer, Lambda 35, UV/Vis Spectrometer-Integrated Sphere.

3. Computational details

The calculations were performed at DFT levels on a Pentium 1V/3.02 GHz personal computer using Gaussian 03W [21] program package, invoking gradient geometry optimization [21,22]. In order to establish the stable possible conformations, the conformational space of title compound was scanned with molecular mechanic simulations. This calculation was performed with the Spartan 08 program [23]. For meeting the requirements of both accuracy and computing economy, theoretical methods and basis sets should be considered. Density functional theory (DFT) has been proved to be extremely useful in treating electronic structure of molecules. The basis set 6-311++G(d,p) was used for the conformational analysis. The optimized structural parameters were used in the vibrational frequency calculations at the DFT level to characterize all stationary points as minima. Then, vibrationally averaged nuclear positions of (*E*)-2-HBAPPA were used for harmonic vibrational frequency calculations resulting in IR and Raman frequencies together with intensities and Raman depolarization ratios. In the present work, the DFT method B3LYP/6-311++G(d,p) were used for the computation of molecular structure, vibrational frequencies and energies of optimized structures. The vibrational modes were assigned on the basis of TED analysis for higher basis set (B3LYP/6-311++G(d,p)), using SQM program [24].

It should be noted that Gaussian 03W package able to calculate the Raman activity. The Raman activities were transformed into Raman intensities using Raint program [25] by the expression:

$$I_i = 10^{-12} \times (\nu_0 - \nu_i)^4 \times \frac{1}{\nu_i} \times RA_i \qquad (1)$$

where I_i is the Raman intensity, RA_i is the Raman scattering activities, ν_i is the wavenumber of the normal modes and ν_0 denotes the wavenumber of the excitation laser [26].

4. Results and discussion

4.1. Molecular geometry

The numbering scheme for (*E*)-2-HBAPPA is shown in Fig. 1 Optimized bond parameters were calculated by using B3LYP with 6-311++G(d,p) basis set. To find stable conformer, a meticulous conformational analysis was carried out for the title compound. Rotating 10 each degree intervals around the free rotation bonds, conformational space of the title compound was scanned by molecular mechanic simulations and then full geometry optimizations of these structures were performed by B3LYP/6-311++G(d,p) method. Results of geometry optimizations were indicated that the title compound is rather flexible molecule and, in theory, may have at least 16 conformers are shown in Fig. 2. Ground state energies, zero point corrected energies (Eelect. + ZPE), relative energies and dipole moments of conformers were presented in Table 1. Zero point corrections have not caused any significant changes in the stability order.

The optimized geometrical parameters are calculated using B3LYP/6-311++G(d,p) basis set and also listed in the Table 2. In the present work, the introduction of hydroxyl group in the phenyl ring causes some changes in the C—C and C═C bond lengths. As it is evident from the NBO analysis, the bond distance of $C_1—C_2$ (1.401), $C_3—C_4$ (1.407), $C_5—C_6$ (1.401) and $C_2—C_3$ (1.420), $C_4—C_5$ (1.384), $C_1—C_6$ (1.387 Å) are belongs to C—C and C═C bonds, respectively. In which C═C bond distance is lesser than C—C bond with an exception, which ($C_2—C_3$) may be due to the formation of intramolecular hydrogen bond between $N_{23}\cdots H_{22}$. The $C_{14}—C_{25}$ bond distance (1.514 Å) is greater than the $C_3—C_{11}$ (1.452 Å) bond. The reason may also be due to formation of $N_{23}\cdots H_{22}$. The increase of $C_2═C_3$ bond length is due to transfer of lone pair of electron from LPO_{21} to $C_2—C_3$, which accept 33.26 kJ/mol energy during the intramolecular interaction, through $n \rightarrow \pi^*$ transition. This $C_2—C_3$ bond length is supported from the literature [27,28].

The bond distance of $C_{13}—N_{23}$ and $C_{11}═N_{23}$ are calculated about 1.461 and 1.284 Å respectively, using B3LYP/6-311++G(d,p) level. These values are in agreement with X-ray diffraction data of Khalaji et al. [27]. The carbonyl group ($C_{17}═O_{18}$) bond length 1.203 Å B3LYP/6-311++G(d,p) is shorter than $C_{17}—O_{19}$ (1.353 Å). This is due to π electron localization in C═O. The intra-molecular interaction between nitrogen and hydrogen ($H_{22}\cdots N_{23}$) of OH group is calculated as 1.758 Å. This is further supported by increasing and decreasing the bond length of $O_{21}—H_{22}$ and $C_2—O_{21}$ respectively.

It is evident from the Table S1; the $C_2—O_{21}—H_{22}$ bond angle is positively deviated (~0.50°) from $C_{17}—O_{19}—H_{20}$, which is due to $N_{23}\cdots H_{22}$. The highest bond angle 125.82° is observed for

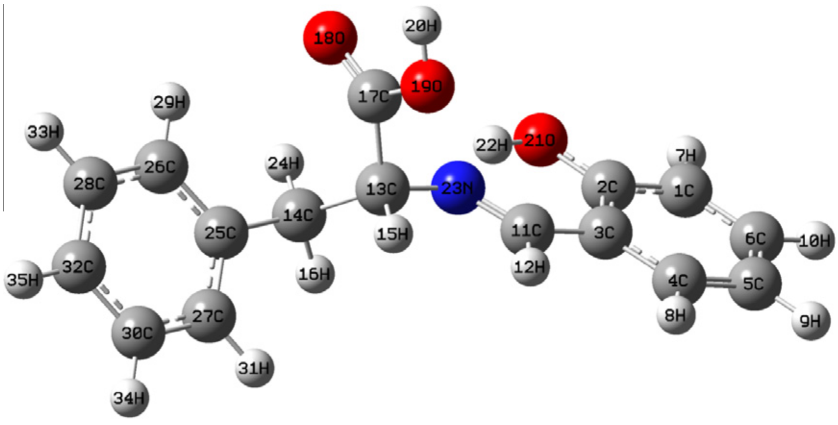

Fig. 1. The optimized structure of (*E*)-2-(2-hydroxy benzylidene amino)-3-phenyl propionic acid (*E*)-2HBAPPA.

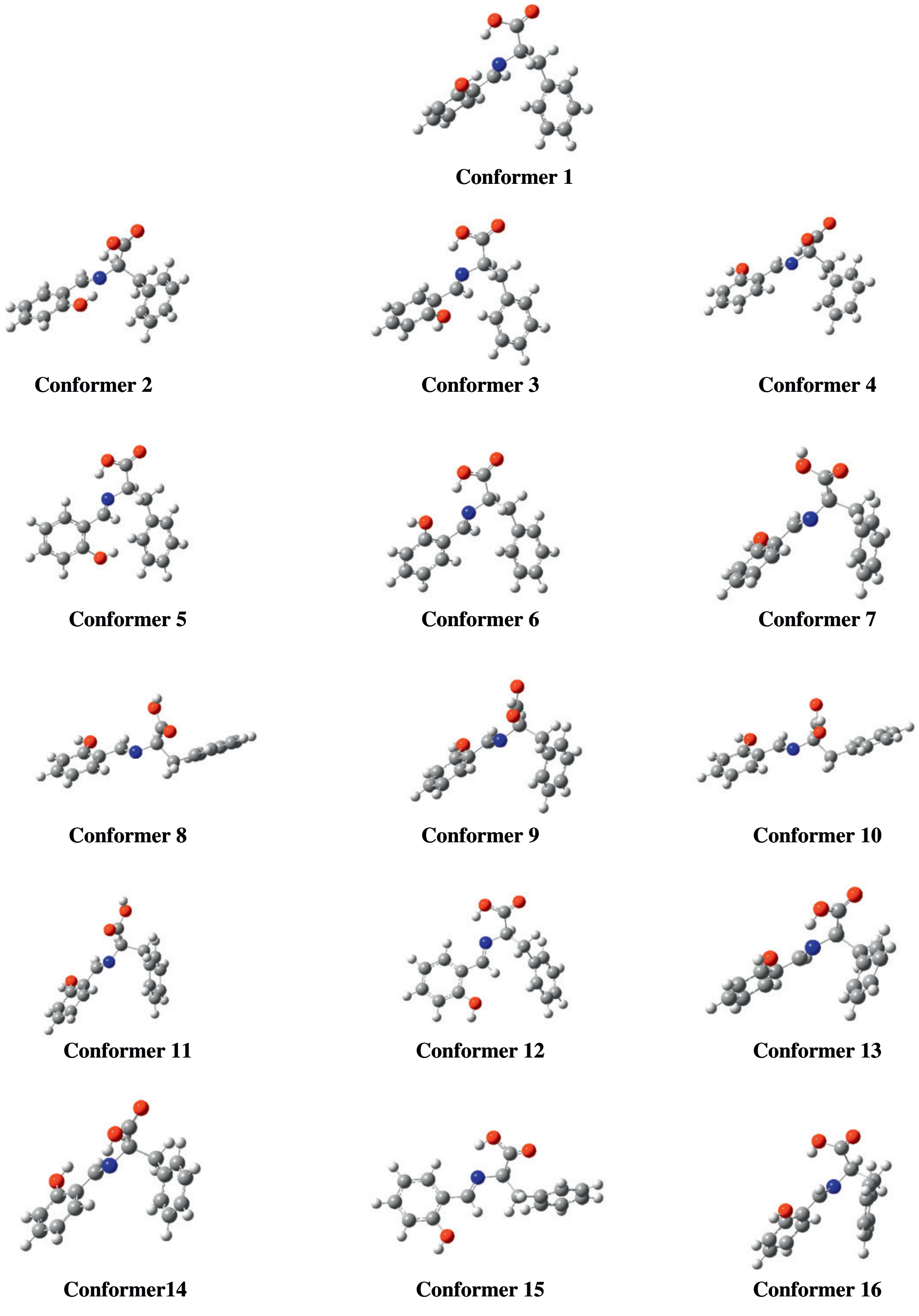

Fig. 2. All possible conformers of (*E*)-2HBAPPA.

C_{13}—C_{17}—O_{18} while C_3—C_2—O_{21} has lower value 122.05°. This is also due to the formation of hydrogen bond. The above mentioned bond angles are comparable with Wang et al. [28] and Choudhury and Guru Row [29]. All the possible bond parameters are listed in Table S1.

4.2. Vibrational assignments

The molecule (*E*)-2-HBAPPA contains carboxylic, hydroxyl, methylene and amino groups. It also consists of 35 atoms, hence one can have 99 normal modes of vibrations. The harmonic wavenumber calculations were performed with B3LYP/6-311++G(d,p) level basis sets. The title molecule belongs to C_1 point group symmetry. The recorded FT-IR, FT-Raman and calculated wavenumbers, intensities (IR, Raman), force constant and reduced mass are given in Table 2. The comparisons of experimental and theoretical spectra are shown in Fig. 3 (FT-IR), and Fig. 4 (FT-Raman). The total energy distributions for all fundamental vibrations were calculated using scaled quantum mechanics (SQMs) method at B3LYP/6-311++G(d,p) level [24].

4.2.1. O—H vibrations

The O—H vibrations are extremely sensitive to formation of hydrogen bonding [30]. The O—H stretching band is characterized

Table 1
Energetics of the conformers calculated at the B3LYP/6-311++G(d,p) level for (*E*)-2-HBAPPA.

Conformers	*E* (Hartree)	Δ*E* (kcal/mol)	E_0 (Hartree)	ΔE_o (kcal/mol)	Dip. Mom. (D)
1	−899.4276787	0.000	−899.148553	0.000	5.734
2	−899.4258804	1.128	−899.146749	1.132	5.1314
3	−899.4176265	6.308	−899.139411	5.737	7.9904
4	−899.4154509	7.673	−899.137339	7.037	7.7469
5	−899.4153587	7.731	−899.13686	7.337	5.3891
6	−899.4146429	8.180	−899.136406	7.622	7.4491
7	−899.4136486	8.804	−899.13604	7.852	4.4509
8	−899.4135281	8.880	−899.135776	8.018	4.351
9	−899.4132263	9.069	−899.135494	8.195	3.4047
10	−899.412589	9.469	−899.134915	8.558	3.1123
11	−899.4125709	9.480	−899.135061	8.466	3.3276
12	−899.4120259	9.822	−899.133875	9.211	7.912
13	−899.4116909	10.032	−899.133507	9.442	7.3625
14	−899.4114878	10.160	−899.133433	9.488	4.9419
15	−899.4090454	11.693	−899.131027	10.998	7.2872
16	−899.4034218	15.221	−899.125329	14.573	5.5116

E_o, zero point corrected energy, (Dip.Mom. – dipole moment).

by a very broad band appear in the range 3400–3600 cm^{-1} [31]. Stretching of O—H band is characterized by a very broad band appear at 3400 cm^{-1} by Meganathan et al. [32]. In the present investigation, the O—H stretching band is recorded at 3293 and 3435 cm^{-1} as weak broad band using FT-IR whereas there is no Raman counterpart. The calculated hydroxyl group, stretching vibration appeared at 3144 and 3626 cm^{-1} (mode nos: 98, 99) by using B3LYP/6-311++G(d,p) basis set. The TED values 90% support the present assignments.

Krishnakumar and Mathammal [33], have studied the in-plane bending vibration of O—H appeared at 1463, 1294, 1160 cm^{-1} 1340 cm^{-1}, while the Sundaraganesan et al. [34] and Selverstein et al. [35], were recorded in the range of 1440–1395 cm^{-1}. In the present work, the O—H in-plane bending modes observed at 1413 (strong) in FT-IR and 1413 (medium) in FT-Raman spectra. This mode is appeared with the mixer of C—C—H vibrations and their contributions are 31 and 10 for 73 and 64 mode numbers, respectively. These assignments are further supported by harmonic values. Out-of-plane bending mode of OH group appeared at 745 (strong) and 747 cm^{-1} (medium) band in FT-IR and FT-Raman spectra, respectively. The calculated Γ_{O-H} values 746, 818 cm^{-1} (mode nos: 34, 38/B3LYP/6-311++G(d,p)) are well coincide with the experimental and literature values [36].

4.2.2. C—H vibrations

The phenyl ring C—H vibration is observed at 3095 cm^{-1} as broad and low intense band in FT-IR spectrum [37]. In (*E*)-2-HBAPPA molecule, the carbon bonded hydrogen atom stretching vibrations are observed at 3084, 3067, 3063 cm^{-1} as medium strong band in FT-IR and 3064 cm^{-1} (strong) in FT-Raman. The computed wavenumbers for the same mode are assigned in the range of 3092–3045 cm^{-1}/B3LYP/6-311++G(d,p)/mode nos: 97–89. In which mode nos: 97 (sym), 94 (asym) and 95 (sym), 96 (asym) are belongs to C—H stretching vibrations in phenyl and phenol rings respectively. The observed bands 2925 (FT-IR)/2925 (FT-Raman) and 2866 (FT-IR)/2864 (FT-Raman) are belongs to $C_{11}—H_{12}$ and $C_{13}—H_{15}$ stretching vibrations, which are supported by TED and harmonic values (B3LYP/6-311++G(d,p)/mode nos: 86, 85). These assignments are also find support from Wang et al. [28].

In the present study, the FT-IR/FT-Raman bands at 1311, 1209, 1154, 1130/1312, 1216, 1159 cm^{-1} and at 912, 851/851, 831 cm^{-1}, respectively in (E)-2-HBAPPA have been designated to δ_{C-H} and Γ_{C-H} modes. In aromatic compounds, the C—H in-plane bending wavenumber appeared in the range of 1000–1300 cm^{-1} and C—H out-of-plane bending vibration appeared in the range of 750–1000 cm^{-1} [34,36]. In (*E*)-2-(2-hydroxy benzyliden amino)-3-methyl butanoic acid ((*E*)-2HBAMBA), the C—H in-plane bending vibration has appeared at 1295, 1294, 1236, 1181, 1140 and 1074 cm^{-1} in FT-IR spectrum. Similarly, the observed bands 942, 833, 746: FT-IR and 964, 946 cm^{-1}: FT-Raman are assigned to Γ_{C-H} mode. The scaled vibrations are at 1310, 1219, 1164, 1139 and 971, 956, 922, 844, 831 cm^{-1} (B3LYP/6-311++G(d,p)/mode nos: 68, 63, 59, 57 and 47, 46, 43, 40, 39) correspond to δ_{C-H} and Γ_{C-H} respectively. These assignments are in the expected range and also find support from the literature [35]. The observed as well as calculated values are find support from the ((*E*)-2HBAMBA) [37]. The mode nos: 72 (1369 cm^{-1})/48 (979 cm^{-1}) are belongs to $\delta C_{11}—H_{12}$/$\Gamma C_{11}—H_{12}$ mode respectively.

4.2.3. Methylene group vibrations

For the assignment of CH_2 group frequencies basically six fundamentals can be associated to each CH_2 group namely, CH_2 symmetric, CH_2 asymmetric, scissoring and rocking, which belong to in-plane vibration. In addition to that, CH_2 wagging and twisting modes of CH_2 groups would be expected to be depolarized for out-of-plane symmetry species. The CH_2 asymmetric stretching vibrations are generally observed in the region 3100–3000 cm^{-1}, while the symmetric stretching appears between 3000 and 2900 cm^{-1} [38–41]. For (*E*)-2-HBAPPA, the recorded FT-IR and FT-Raman were shown peaks belongs to CH_2 symmetric stretching at 2956 (medium) and 2964 cm^{-1} (weak) respectively, whereas the asymmetric stretching mode appeared at 3007 cm^{-1} (FT-IR: medium) and 3009 cm^{-1} (FT-Raman: weak). The theoretical calculation for CH_2 symmetric and asymmetric vibrations appeared at 2951 and 3001 cm^{-1} (mode no: 87, 88) respectively, by using B3LYP/6-311++G(d,p) basis sets. From these observations, the methylene group stretching values are correlated well with the theoretical values and also agree well with above literature values. The TED values are also support the assignments.

The scissoring mode of CH_2 group gives rise to a characteristic band near 1415 cm^{-1} in FT-IR and 1400 cm^{-1} in Raman spectra. The twisting, wagging and rocking vibration appears in the region 1400–900 cm^{-1} [42]. The observed band at 1444 cm^{-1} (both FT-IR and FT-Raman) and the corresponding calculated wavenumber for this mode at 75, is 1439 cm^{-1}/B3LYP/6-311++G(d,p) are attributed CH_2 scissoring vibration. This is supported by TED value (16%). The wagging and rocking modes are calculated at 69 and 9. The observed FT-IR 146 cm^{-1} as a very strong band assigned to CH_2 rocking. These assignments are comparable with the literature [43] and also find support from TED.

Table 2
Vibrational wave numbers obtained for (*E*)-2-HBAPPA at B3LYP/6-311++G(d,p) [harmonic frequency (cm^{-1}), IR, Raman intensities (km/mol)].

Mode no.	Calculated and observed frequencies (cm^{-1})[a]			Intensities		Vibrational assignments TED ⩾ 10%[d]
	6-311++G(d,p)	FT-IR	FT-Raman	IR_c[b]	RS_c[c]	
ν_1	21			0.03	74.62	$\Gamma_{C11N23C13C14}(14) + \Gamma_{C25C14C13N23}(18)$
ν_2	28			0.12	51.92	$\Gamma_{C11N23C13C14}(20) + \Gamma_{C11N23C13H15}(16) + \Gamma_{C11N23C13C17}(24)$
ν_3	37			0.00	24.99	$\Gamma_{C13N23C11C3}(19)$
ν_4	43			0.32	31.09	$\Gamma_{O18C17C13N23}(21) + \Gamma_{O19C17C13N23}(27)$
ν_5	54			0.06	33.10	$\delta_{C25C14C13}(10) + \Gamma_{C27C25C14C13}(16) + \Gamma_{C27C25C14H24}(12)$
ν_6	79			0.19	17.23	$\Gamma_{C25C14C13C17}(14)$
ν_7	103			0.12	5.35	$\delta_{N23C11C3}(17) + \delta_{C11N23C13}(13)$
ν_8	116		126vs	0.07	11.20	$\Gamma_{N23C11C3C4}(17) + \Gamma_{C11-N23-C13-C17}(10)$
ν_9	165		143vs	0.12	6.22	$\delta_{C14C13C17}(26) + \Gamma_{C11N23C13C14}(11)$
ν_{10}	205		213m	0.18	1.37	$\Gamma_{C4C3C2O21}(14) + \Gamma_{O21C2C1C6}(13)$
ν_{11}	216			0.01	7.19	$\nu_{CC}(11) + \Gamma_{CCCC}(26)$
ν_{12}	249			0.70	3.34	$\delta_{C4C3C11}(12) + {}_{\delta O18C17C13}(14) + \delta_{O19C17C13}(11)$
ν_{13}	313		317m	1.06	4.18	$\Gamma_{H12C11C3C2}(10) + \Gamma_{N23C11C3C2}(17)$
ν_{14}	333			0.09	2.41	$\Gamma_{C13N23C11C3}(13) +$
ν_{15}	347			0.11	0.44	$\delta_{C26C25C14}(21) + \delta_{C27C25C14}(25)$
ν_{16}	357		367w	0.17	0.74	$\delta_{C11C3C2}(16) + \delta_{C11N23C13}(16)$
ν_{17}	402	410w		0.00	0.15	$\Gamma_{C32C28C26C25}(19) + \Gamma_{C32C30C27C25}(19)$
ν_{18}	418	427w		0.42	2.39	$\delta_{C4C3C11}(11) + \delta_{O19C17C13}(12)$
ν_{19}	446			0.76	2.11	$\nu_{CC}(10) + \delta_{CCC}(10) + \delta_{OCC}(10)$
ν_{20}	452			1.22	2.08	$\delta_{O21C2C1}(28) + \delta_{C3C2O21}(26)$
ν_{21}	457	473s	472m	0.74	0.60	$\Gamma_{CCCC}(23)$
ν_{22}	527	523vs		4.59	1.76	$\delta_{OCC}(16) + \Gamma_{CCCC}(14)$
ν_{23}	542			1.55	1.36	$\Gamma_{C1C6C5C4}(14)$
ν_{24}	551			2.71	5.44	$\delta_{C3C2C1}(11)$
ν_{25}	579			15.61	0.34	$\Gamma_{H20O19C17C13}(18)$
ν_{26}	586			2.88	0.75	$\delta_{CCC}(21)$
ν_{27}	615	606m	605w	0.03	2.43	$\delta_{C28C26C25}(13) + \delta_{C30C27C25}(14) + \delta_{C32C28C26}(16) + \delta_{C32C30C27}(15)$
ν_{28}	621	622w	622m	5.32	2.06	$\delta_{O18C17C13}(13) + \delta_{O18C17O19}(16) + \Gamma_{H20O19C17C13}(17) + \Gamma_{H20O19C17O18}(16)$
ν_{29}	649			0.34	2.60	$\Gamma_{H20O19C17O18}(12)$
ν_{30}	690	679m		8.31	0.08	$\Gamma_{H35C32C28C26}(11) + \Gamma_{H35C32C30C27}(11)$
ν_{31}	722	698s		1.57	0.44	$\Gamma_{C3C2C1H7}(10) + \Gamma_{C11C3C2O21}(11)$
ν_{32}	737			3.24	0.76	$\nu_{CC}(14) + \Gamma_{CCCH}(28)$
ν_{33}	739			13.23	0.31	$\Gamma_{H9C5C4C3}(19) + \Gamma_{C1C6C5H9}(16) + \Gamma_{H10C6C1C2}(11)$
ν_{34}	746	745vs	747m	8.94	1.22	$\Gamma_{H20O19C17O18}(16)$
ν_{35}	772	775s		2.90	10.65	$\nu_{C2C1}(11) + \nu_{C3C2}(21)$
ν_{36}	798			0.63	6.61	$\nu_{C17C13}(18)$
ν_{37}	809			0.85	7.93	$\nu_{C25C14}(17)$
ν_{38}	818			12.86	0.11	$\Gamma_{H22O21C2C1}(41) + \Gamma_{H22O21C2C3}(46)$
ν_{39}	831		831s	0.08	0.14	$\Gamma_{HCCC}(49) + \Gamma_{CCCH}(34) + \Gamma_{HCCH}(16)$
ν_{40}	844	851s	851w	0.15	0.13	$\Gamma_{C5C6C1H7}(13) + \Gamma_{H10C6C5H9}(11) + \Gamma_{O21C2C1H7}(20)$
ν_{41}	876			2.83	0.58	$\delta_{C1C6C5}(13) + \delta_{C6C5C4}(12)$
ν_{42}	901			0.57	0.25	$\Gamma_{H34C30C27H31}(12) + \Gamma_{H35C32C28H33}(10)$
ν_{43}	922	912m		0.06	0.11	$\Gamma_{H9C5C4H8}(33)$
ν_{44}	946			0.44	0.89	$\Gamma_{H33C28C26H29}(16) + \Gamma_{H34C30C27H31}(20)$
ν_{45}	955	947w	954w	0.14	0.09	$\nu_{CC}(13)$
ν_{46}	956			0.01	0.00	$\Gamma_{H10C6C1H7}(30) + \Gamma_{H10C6C5H9}(28)$
ν_{47}	971			0.03	0.02	$\Gamma_{H33C28C26H29}(18) + \Gamma_{H35C32C28H33}(24) + \Gamma_{H35C32C30H34}(18)$
ν_{48}	979			1.12	4.08	$\Gamma_{H12C11C3C2}(12) + \Gamma_{H12C11C3C4}(17) + \Gamma_{C13N23C11H12}(26)$
ν_{49}	984	986m		0.07	16.36	$\nu_{CC}(33) + \delta_{CCC}(42)$
ν_{50}	1013		1005vs	1.44	14.92	$\nu_{C6C1}(10) + \nu_{C6C5}(32)$
ν_{51}	1016			1.18	10.37	$\nu_{C32C28}(23) + \nu_{C32C30}(24)$
ν_{52}	1028			5.63	7.53	$\nu_{C14C13}(33) + \nu_{N23C13}(22)$
ν_{53}	1039	1036m	1035s	5.07	1.83	$\nu_{C14C13}(12) + \nu_{N23C13}(33)$
ν_{54}	1066	1074m		6.01	1.18	$\nu_{C28C26}(13) + \nu_{C30C27}(13) + \delta_{CCH}(31)$
ν_{55}	1102			9.57	0.43	$\nu_{C5C4}(18) + \delta_{H10C6C5}(10)$
ν_{56}	1104			30.87	0.78	$\nu_{O19C17}(35) + \delta_{H20O19C17}(19)$
ν_{57}	1139	1130w		4.08	4.65	$\delta_{H9C5C4}(15) + \delta_{C6C5H9}(14) + \delta_{H10C6C1}(14) + \delta_{H10C6C5}(13)$
ν_{58}	1142			0.11	0.81	$\delta_{H34C30C27}(11) + \delta_{C32C30H34}(10) + \delta_{H35C32C28}(19) + \delta_{H35C32C30}(19)$
ν_{59}	1164	1154ms	1159m	0.12	0.12	$\delta_{H29C26C25}(10) + \delta_{H33C28C26}(10) + \delta_{C32C28H33}(10)$
ν_{60}	1171			9.35	7.03	$\delta_{H20O19C17}(10) + \delta_{H24C14C13}(12)$
ν_{61}	1181		1187w	0.01	8.59	$\nu_{C25C14}(37) + \delta_{CCH}(14)$
ν_{62}	1193			5.28	7.46	$\nu_{C2C1}(22) + \nu_{C11C3}(21)$
ν_{63}	1219	1209m	1216s	2.26	27.61	$\nu_{C4C3}(20) + \delta_{H8C4C3}(17) + \delta_{C5C4H8}(14)$
ν_{64}	1254			0.71	1.31	$\delta_{H20O19C17}(23) + \Gamma_{CCCH}(16)$
ν_{65}	1268			1.56	2.31	$\delta_{H16C14C13}(13) + \delta_{H20O19C17}(14) + \delta_{CCH}(14)$
ν_{66}	1273	1294m		13.42	0.82	$\nu_{O21C2}(39) + \delta_{CCH}(18)$
ν_{67}	1294			0.26	0.64	$\nu_{C26C25}(14) + \nu_{C27C25}(14) + \nu_{C32C28}(10) + \nu_{C32C30}(10)$
ν_{68}	1310	1311w	1312w	0.11	32.25	$\delta_{H29C26C25}(13) + \delta_{C28C26H29}(11) + \delta_{H31C27C25}(13) + \delta_{C30C27H31}(12)$
ν_{69}	1314			1.01	1.89	$\nu_{CC}(19) + \Gamma_{HCCC}(16)$
ν_{70}	1321			0.83	3.24	$\nu_{C3C2}(13) + \nu_{C5C4}(10) + \nu_{C6C1}(11)$
ν_{71}	1347	1341s	1340m	3.37	4.94	$\nu_{O19C17}(11)$
ν_{72}	1369			6.26	4.06	$\delta_{H12C11C3}(11) + \delta_{H12C11N23}(23)$

(*continued on next page*)

Table 2 (*continued*)

Mode no.	Calculated and observed frequencies (cm^{-1})[a]			Intensities		Vibrational assignments TED ⩾ 10%[d]
	6-311++G(d,p)	FT-IR	FT-Raman	IR_c[b]	RS_c[c]	
ν_{73}	1400	1413s	1413m	6.96	6.99	$\nu_{C6C1}(11) + \delta_{H22O21C2}(36)$
ν_{74}	1433			1.11	0.83	$\delta_{H16C14H24}(15)$
ν_{75}	1439	1444w	1444s	1.50	2.71	$\delta_{H16C14H24}(16)$
ν_{76}	1442	1457m		11.67	39.27	$\nu_{C3C2}(14) + \nu_{C5C4}(12) + \nu_{O21C2}(14)$
ν_{77}	1476			2.93	0.39	$\Gamma_{HCCC}(31) + \delta_{CCH}(30)$
ν_{78}	1477	1503vs		6.18	6.18	$\nu_{C6C5}(15) + \delta_{H9C5C4}(11) + \delta_{H22O21C2}(23)$
ν_{79}	1559		1553w	14.21	28.50	$\nu_{C3C2}(11) + \nu_{C6C1}(18) + \nu_{C6C5}(13) + \delta_{H22O21C2}(19)$
ν_{80}	1568			0.20	0.20	$\nu_{C26C25}(16) + \nu_{C27C25}(15) + \nu_{C32C28}(19) + \nu_{C32C30}(20)$
ν_{81}	1589	1587vs	1588m	2.33	11.81	$\nu_{C28C26}(21) + \nu_{C30C27}(22)$
ν_{82}	1606		1606s	20.77	28.63	$\nu_{C2C1}(20) + \nu_{C5C4}(20) + \delta_{H22O21C2}(11)$
ν_{83}	1619	1619vs		60.35	60.35	$\nu_{N23C11}(62)$
ν_{84}	1757	1773w		56.63	1.23	$\nu_{C17{=}O18}(86)$
ν_{85}	2908	2866m	2864w	4.74	2.22	$\nu_{C13H15}(99)$
ν_{86}	2918	2925m	2925s	8.32	2.11	$\nu_{C11H12}(99)$
ν_{87}	2951	2956m	2964w	2.93	2.85	$\nu_{C14H16}(73) + \nu_{C14H24}(27)$
ν_{88}	3001	3007m	3009w	0.97	0.97	$\nu_{C14H16}(27) + \nu_{C14H24}(73)$
ν_{89}	3045	3036m		1.82	1.39	$\nu_{C27H31}(81) + \nu_{C30H34}(16)$
ν_{90}	3054			0.70	1.45	$\nu_{C4H8}(90)$
ν_{91}	3058			0.03	2.56	$\nu_{C28H33}(39) + \nu_{C32H35}(40)$
ν_{92}	3066	3063m	3064vs	1.68	3.47	$\nu_{C6H10}(80)$
ν_{93}	3067	3067m		3.10	3.20	$\nu_{C28H33}(36) + \nu_{C30H34}(43)$
ν_{94}	3077			3.52	1.66	$\nu_{C26H29}(23) + \nu_{C30H34}(29) + \nu_{C32H35}(41)$
ν_{95}	3084	3084m		2.46	9.89	$\nu_{C1H7}(73) + \nu_{C5H9}(12) + \nu_{C6H10}(14)$
ν_{96}	3086			2.48	3.75	$\nu_{C1H7}(19) + \nu_{C5H9}(67)$
ν_{97}	3092			1.48	9.29	$\nu_{C26H29}(63) + \nu_{C28H33}(20)$
ν_{98}	3144	3293w		100.00	3.77	$\nu_{O21H22}(93)$
ν_{99}	3626	3435w		13.94	2.70	$\nu_{O19H20}(100)$

ν: Stretching, δ: bending, Γ: Torsion, vw: very week, w: week, m: medium, s: strong, vs: very strong.

[a] Calculated and observed vibrational frequencies [scaling factor: 0.9608].

[b] Relative IR absorption intensities normalized with highest peak absorption equal to 100.

[c] Relative Raman intensities calculated by Eq. (1) and normalized to 100.

[d] Total energy distribution calculated B3LYP 6-311++G(d,p) level, TED less than 10% are not shown.

4.2.4. C=O, C—O vibrations

Vibrational analysis of carboxylic acid is made on the basis of carbonyl and hydroxyl group. The carbonyl stretching frequency has been most extensively studied by infrared spectroscopy [43]. This multiply bonded group is highly polar and therefore gives rise to an intense infrared absorption band. The carbon–oxygen double bond is formed by p_π–p_π bonding between carbon and oxygen. Because of the different electro negativities of carbon and oxygen atoms, the bonding electrons are not equally distributed between the two atoms. The following two resonance forms contribute to the bonding of the carbonyl group $>C{=}O \leftrightarrow C^{+}{-}O^{-}$. The lone pair of electrons on oxygen also determines the nature of the carbonyl group. As discussed earlier in the geometry of the molecule, due to the intra-molecular hydrogen bond existing among the carbonyl and hydroxyl group, the C=O stretching wave number shifts to a lower value typically absorbs very strongly in the 1660–1715 cm^{-1} region [44].

In (*E*)-2-HBAPPA, the band appeared at 1773 cm^{-1} as weak band in FT-IR is belongs to C=O group, while the Raman counterpart is absent. The corresponding calculated wavenumber is at 1757 cm^{-1} (mode nos: 84). The experimental wavenumber for C=O is slightly deviated by the theoretical value this is due to intermolecular interaction in the solid phase. This assignment is in line with the assignment proposed by literature [44] and also supported from TED value (86%). The bond C—O (carboxylic group) stretching vibration is observed at 1341 cm^{-1} (strong: FT-IR)/1340 cm^{-1} (medium: FT-Raman), which is in consistent with theoretical wavenumber 1347 cm^{-1} using B3LYP/6-311++G(d,p) basis set (mode no: 71). The substituted hydroxyl oxygen and ring carbon (C_2—O_{21}) stretching mode has calculated at 1273 cm^{-1} using B3LYP/6-311++G(d,p) (mode no: 66).

The calculated as well as observed wavenumbers 1294 cm^{-1}/FT-IR for $\nu_{(C—O)}$ coincide well with the assignment proposed by Subramanian et al. [45]. The $\nu_{(C17—O19)}$ in carboxylic group is observed at higher frequency (mode no: 71/1347 cm^{-1}) than the $\nu_{(C2—O21)}$. It may be due to the resonance in phenol ring [46]. The calculated frequency of the C—O—H (carboxylic group) in-plane and out-of-plane bending vibrations in (*E*)-2-HBAPPA (mode nos: 64 and 34) are 1254 and 746 cm^{-1}, respectively. In which Γ_{COOH} values is well supported by experimental observations (745: FT-IR/747 cm^{-1}: FT-Raman). The δ_{COH} (ring) vibration has been assigned to a strong band at 1413 cm^{-1} (both FT-IR/FT-Raman) of (*E*)-2-HBAPPA, and this is supported by our calculation (1400 cm^{-1} B3LYP/6-311++G(d,p)/mode no: 73). The wave number 818/6-311++G(d,p) mode no: 38 is attributed to COH (ring) out-of-plane bending. These assignments are supported by literature [47]. According to our calculations, the δ_{CCO} (carboxylic) vibration (621 cm^{-1} B3LYP/6-311++G(d,p) mode no: 28) assigned to a weak FT-IR/medium intensity Raman band at about 622 cm^{-1}. The mode number 4 is assigned to Γ_{CCO} mode (carboxylic). The calculated wavenumbers 452 and 205 cm^{-1} (B3LYP/6-311++G(d,p) mode nos: 20, 10) are assigned to δ_{CCO} and Γ_{CCO} vibrations respectively.

4.2.5. C=N, C—N vibrations

The identification of C=N and C—N vibrations are the very difficult task, since the mixing of several bands are possible in the region [35]. The C=N stretching appears in the region 1600–1670 cm^{-1} [47]. Wang et al. [28] have assigned at 1633 cm^{-1} (FT-IR) and 1625 cm^{-1} (FT-Raman) to aforementioned band. The C=N (aromatic) stretching mode appeared in the region 1490–1570 cm^{-1} [27]. In the present study, C=N bond stretching vibration is observed at 1619 cm^{-1} (as very strong) in FT-IR spectrum, while there is no Raman counterpart. The calculated C=N group frequency 1619 cm^{-1} (mode no: 83) using B3LYP/6-311++G(d,p) basis set coincide well with the experimental data and also supported by TED (62%) value. In the present work, the bands

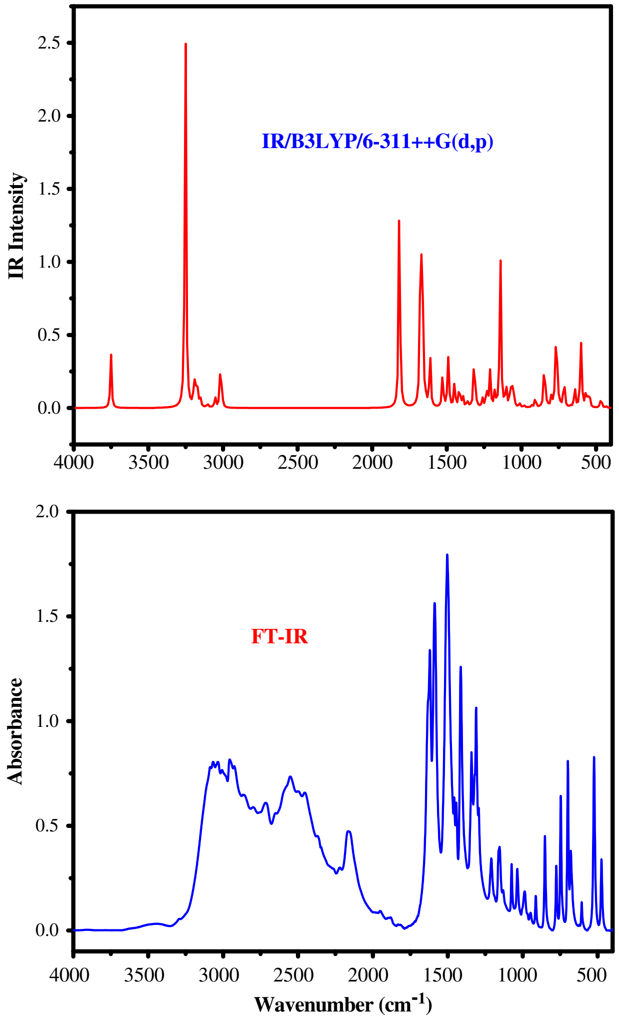

Fig. 3. The experimental and theoretical FT-IR spectra of (*E*)-2HBAPPA.

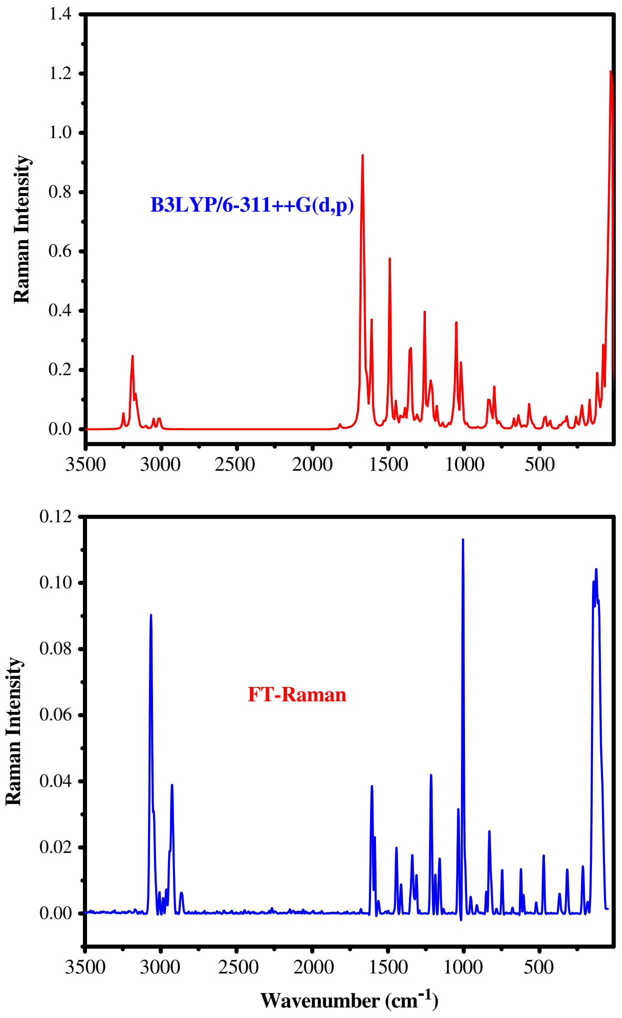

Fig. 4. The experimental and theoretical FT-Raman spectra of (*E*)-2HBAPPA.

identified at 357 and 165 cm^{-1} (B3LYP/6-311++G(d,p) mode nos: 16, 9) have been designated to $\delta_{C=N-C}$ and $\Gamma_{C=N-C}$ modes, respectively by consideration of their corresponding experimental (367 and 143 cm^{-1} Raman, respectively) assignments. The calculated wave numbers 1369 and 979 cm^{-1} (B3LYP/6-311++G(d,p) mode nos: 72, 48) are attributed $\delta_{N=C-H}$ and $\Gamma_{N=C-H}$ vibrations respectively.

In this work, the band occurs at 1036 in FT-IR and at 1035 cm^{-1} in FT-Raman are assigned to the $\nu_{C13-N23}$ stretching. The wavenumber 1039 cm^{-1} (mode no: 53) is calculated through B3LYP/6-311++G(d,p) is assigned to the ν_{C-N} mode with TED value (33%). Selverstein et al. [35] assigned C—N stretching absorption in the region 1382–1266 cm^{-1} for aromatic amines. For (*E*)-2-HBAPPA, the ν_{C-N} vibration is observed at lower frequency than the literature value, which may be due to the formation of intra-molecular hydrogen bond between $N_{23}\cdots H_{22}$. Similar observation has been observed for *ortho*-hydroxy acylaromatic Schiff base by Pajak et al. [48].

4.2.6. C=C, C—C vibrations

In our present study, the C=C stretching vibrations observed at 1606 (strong), 1588 (medium) and 1553 cm^{-1} (weak) in FT-Raman and 1587 cm^{-1} (strong) in FT-IR spectra. As it evident from the Table 2, the modes no: 82, 81, 79 (B3LYP/6-311++G(d,p)) are in agreement with experimental observation and also find support from literature [49].

Table 3
The electric dipole moment (μ), polarizability (α) and hyperpolarizability components (β_0 in × 10^{-30} esu) of (*E*)-2HBAPPA.

Parameters	B3LYP/6-311++G(d,p)
μ (Debye)	1.358
α	5.456
β_{xxx}	−443.64
β_{xxy}	−40.70
β_{xyy}	42.14
β_{yyy}	−117.17
β_{xxz}	255.32
β_{xyz}	−31.38
β_{yyz}	68.84
β_{xzz}	−2.90
β_{yzz}	−26.66
β_{zzz}	104.35
β_0	5.334

In-plane carbon bending vibrations are obtained from the nondegenerate band at 1010 cm^{-1} (b_{1u}) and degenerate modes 606 cm^{-1} (e_{2g}) of benzene. Likewise, the C—C—C out-of-plane bending modes are defined with reference to 703 cm^{-1} (b_{2g}) and degenerate 404 cm^{-1} (e_{2u}) modes of benzene, Belemy [50]. A major coincidence of theoretical values with that of experimental evaluation is found in the δ_{C-C-C} and $\Gamma_{C-C-C-C}$ vibrations. The C—C in-plane bending and C—C—C out-of-plane bending vibrations are ob-

Table 4
Second order perturbation theory analysis of Fock matrix in NBO basis (*E*)-2HBAPPA.

Type	Donor (i)	ED/e	Acceptor (*j*)	ED/e	$^{a}E^{(2)}$ (kJ/mol)	$^{b}E(j)-E(i)$ (a.u)	$^{c}F(i,j)$ (a.u)
$\sigma-\sigma^*$	$C_1-C_{2(1)}$	1.978	C_1-C_6	0.013	9.96	1.29	0.049
			$O_{21}-H_{22}$	0.073	8.12	1.14	0.042
$\sigma-\sigma^*$	$C_1-C_{6(1)}$	1.979	C_1-C_2	0.024	9.54	1.26	0.048
			C_2-O_{21}	0.019	14.52	1.1	0.055
			C_5-C_6	0.016	10.33	1.27	0.05
$\pi-\pi^*$	$C_1-C_{6(2)}$	1.700	$C_4-C_{5(2)}$	0.313	67.24	0.28	0.061
	C_1-H_7	1.979	C_2-C_3	0.037	18.24	1.05	0.061
			C_5-C_6	0.016	15.65	1.08	0.057
$\sigma-\sigma^*$	$C_2-C_{3(1)}$	1.975	C_1-C_2	0.024	11.88	1.25	0.053
			C_3-C_4	0.020	14.14	1.26	0.058
			C_3-C_{11}	0.026	9.58	1.19	0.047
$\sigma-\sigma^*$	C_2-O_{21}	1.995	C_1-C_6	0.309	5.56	1.51	0.04
			C_3-C_4	0.020	5.94	1.48	0.041
$\sigma-\sigma^*$	C_3-C_4	1.973	C_2-O_{21}	0.019	14.43	1.09	0.055
			$C_{11}-N_{23}$	0.009	7.74	1.3	0.044
$\sigma-\sigma^*$	C_3-C_{11}	1.974	$C_{11}-N_{23}$	0.009	7.95	1.29	0.044
			$C_{13}-N_{23}$	0.027	18.12	1.04	0.06
$\sigma-\sigma^*$	C_4-C_5	1.980	C_3-C_{11}	0.026	13.10	1.19	0.055
$\pi-\pi^*$	$C_4-C_{5(2)}$	1.708	C_1-C_6	0.013	91.67	0.29	0.071
$\sigma-\sigma^*$	C_4-H_8	1.981	C_2-C_3	0.037	18.49	1.06	0.061
			C_5-C_6	0.016	14.73	1.09	0.055
$\sigma-\sigma^*$	$C_{11}-N_{23(1)}$	1.988	$C_{13}-C_{17}$	0.080	16.61	0.68	0.047
$\pi-\pi^*$	$C_{11}-N_{23(2)}$	1.942	$C_{17}-O_{18}$	0.023	6.32	0.34	0.021
$\sigma-\sigma^*$	$C_{13}-C_{17(1)}$	1.966	$C_{11}-N_{23}$	0.009	4.44	1.25	0.033
			$C_{11}-N_{23}$	0.179	9.79	0.65	0.036
			$O_{19}-H_{20}$	0.015	12.43	1.06	0.05
$\sigma-\sigma^*$	$C_{13}-N_{23(1)}$	1.988	C_3-C_{11}	0.026	16.57	1.23	0.062
			$C_{11}-N_{23(1)}$	0.009	4.52	1.34	0.034
$\pi-\pi^*$	$C_{13}-N_{23(2)}$	1.942	$C_{17}-O_{18}$	0.023	11.05	0.73	0.041
$\sigma-\sigma^*$	$C_{14}-C_{25}$	1.975	$C_{13}-N_{23}$	0.027	8.91	0.97	0.041
			$C_{25}-C_{26}$	0.023	8.62	1.2	0.044
			$C_{25}-C_{27}$	0.023	8.28	1.19	0.043
			$C_{26}-C_{28}$	0.015	9.25	1.2	0.046
			$C_{27}-C_{30}$	0.015	9.41	1.2	0.047
$\sigma-\sigma^*$	$C_{17}-O_{18}$	1.997	$C_{13}-C_{17}$	0.080	4.60	1.45	0.036
			$C_{13}-N_{23}$	0.027	8.12	0.75	0.034
$\sigma-\sigma^*$	$C_{17}-O_{19}$	1.996	$C_{13}-C_{14}$	0.027	4.39	1.31	0.033
$\sigma-\sigma^*$	$O_{19}-H_{20}$	1.986	$C_{13}-C_{17}$	0.080	19.58	1.1	0.065
$\sigma-\sigma^*$	$O_{21}-H_{22}$	1.985	C_1-C_2	0.024	22.89	1.29	0.075
$\pi-\pi^*$	$C_{25}-C_{26(2)}$	1.651	$C_{27}-C_{30}$	0.333	84.85	0.28	0.067
			$C_{28}-C_{32}$	0.332	86.86	0.28	0.068
$\sigma-\sigma^*$	$C_{27}-C_{30(1)}$	1.980	$C_{14}-C_{25}$	0.020	13.93	1.11	0.054
$\pi-\pi^*$	$C_{27}-C_{30(2)}$	1.674	$C_{25}-C_{26}$	0.343	85.06	0.29	0.068
			$C_{28}-C_{32}$	0.332	82.51	0.28	0.067
$\sigma-\sigma^*$	$C_{27}-H_{31}$	1.982	$C_{25}-C_{26}$	0.023	16.57	1.1	0.059
			$C_{30}-C_{32}$	0.016	14.64	1.1	0.055
$\sigma-\sigma^*$	$C_{28}-C_{32}$	1.981	$C_{26}-C_{28}$	0.015	10.63	1.27	0.051
$\pi-\pi^*$	$C_{28}-C_{32(2)}$	1.663	$C_{25}-C_{26}$	0.343	84.10	0.28	0.068
			$C_{27}-C_{30}$	0.333	87.07	0.28	0.068
	$_{LP*}C_2$	0.917	C_1-C_6	0.013	219.37	0.15	0.101
$n-\pi^*$	$_{LP}C_{3(2)}$	1.109	$C_4-C_{5(2)}$	0.313	282.46	0.15	0.106
			$C_{11}-N_{23(2)}$	0.179	291.16	0.12	0.102
$n-\pi^*$	$_{LP}O_{18(2)}$	1.974	$C_{13}-C_{17}$	0.080	85.52	0.62	0.102
			$C_{17}-O_{19}$	0.206	140.79	0.62	0.13
$n-\sigma^*$	$_{LP}O_{19(1)}$	1.976	$C_{17}-O_{18}$	0.023	31.25	1.21	0.085
$n-\pi^*$	$_{LP}O_{19(2)}$	1.812	$C_{17}-O_{18}$	0.206	202.92	0.34	0.116
	$_{LP}O_{21}$	1.972	C_2-C_3	0.037	33.26	1.08	0.083
	$_{LP}N_{23}$	1.866	C_3-C_{11}	0.026	9.46	0.87	0.041
			$C_{11}-H_{12}$	0.036	45.15	0.8	0.085
			$C_{13}-H_{15}$	0.028	21.55	0.8	0.059
			$O_{21}-H_{22}$	0.073	120.00	0.81	0.139

[a] *E*(2) means energy of hyperconjucative interactions (stabilization energy).
[b] Energy difference between donor and acceptor *i* and *j* NBO orbitals.
[c] *F*(*i*, *j*) is the Fock matrix element between *i* and *j* NBO orbitals.

served in FT-IR at 986, 606 (605 cm^{-1}: FT-Raman) and 523, 410 cm^{-1}, respectively. The corresponding calculated frequencies are identified at 984, 615 and 527, 402 cm^{-1}, respectively, (B3LYP/6-311++G(d,p) mode nos: 49, 27 and 22, 17). These assignments are supported by above literature and their corresponding TED values are 42%, 13% and 14%, 19%, respectively. The bands observed in FT-IR: 1036 cm^{-1} (medium)/FT-Raman: 1035 cm^{-1} (strong) and the calculated frequency: 1039 cm^{-1} (B3LYP/6-311++G(d,p) mode no: 53) are assigned to $\nu_{C14-C13}$. The mode no: 50 B3LYP/6-311++G(d,p): 1013 cm^{-1} is attributed to ring breathing vibration, which is supported by FT-Raman band (1005 cm^{-1}) and TED value (42%). In these assignments, the B3LYP/6-311++G(d,p) values are in agreement with experimental values.

Table 5
The electronic transition of (*E*)-2-HBAPPA.

Calculated at B3LYP/6-31G(d,p)	Oscillator strength	Experimental band gap (nm)	Calculated band gap (eV/nm)
Excited state 1	Singlet-A/f = 0.1449	314.65	3.8877 eV/318.91 nm
68 → 76 ($HOMO_{-3}$–$LUMO_{-4}$)	−0.10905		−6.6965
71 → 72 (HOMO–LUMO)	0.64785		−4.4094
Excited state 2	Singlet-A/f = 0.0747	276.32	4.4806 eV/276.72 nm
67 → 72 ($HOMO_{-4}$–LUMO)	0.13860		−5.9512
70 → 72 ($HOMO_{-1}$–LUMO)	0.67754		−4.9867
Excited state 3	Singlet-A/f = 0.0004	254.11	4.6877 eV/264.49 nm
67 → 72 ($HOMO_{-4}$–LUMO)	−0.35405		−5.9511
69 → 72 ($HOMO_{-2}$–LUMO)	0.59207		−5.1656

4.3. Hyperpolarizability calculation

The electric dipole moment (μ), polarizability (α) and first hyperpolarizability (β_0) of (*E*)-2-HBAPPA is calculated using B3LYP/6-311++G(d,p) basis set, based on the finite-field approach. In the presence of an applied electric field, the energy of a system is a function of the electric field. First hyperpolarizability is a third rank tensor that can be described by a 3 × 3 × 3 matrix. The 27 components of the 3D matrix can be reduced to 10 components due to Kleinman symmetry [51]. It can be given in the lower tetrahedral format. It is obvious that the lower part of the 3 × 3 × 3 matrix is a tetrahedral. The components of β are defined as the coefficients in the Taylor series expansion of the energy in the external electric field. When the external electric field is weak and homogeneous, this expansion becomes:

$$E = E^0 - \mu_\alpha F_\alpha - 1/2\alpha_{\alpha\beta}F_\alpha F_\beta - 1/6\beta_{\alpha\beta\gamma}F_\alpha F_\beta F_\gamma \tag{3}$$

where E^0 is the energy of the unperturbed molecules, F_α the field at the origin, and μ_α, $\alpha_{\alpha\beta}$, $\beta_{\alpha\beta\gamma}$ are the components of the dipole moment, polarizability and the first hyperpolarizabilities, respectively. The total static dipole moment μ, the mean polarizability α_0, the anisotropy of polarizability $\Delta\alpha$ and the mean first hyperpolarizability β_0, using the *x*, *y*, *z* components are defined as

$$\mu = \left(\mu_x^2 + \mu_y^2 + \mu_z^2\right)^{1/2} \tag{4}$$

$$\alpha_0 = \frac{\alpha_{xx} + \alpha_{yy} + \alpha_{zz}}{3} \tag{5}$$

$$\Delta\alpha = 2^{-1/2}\Big[(\alpha_{xx} - \alpha_{yy})^2 + (\alpha_{yy} - \alpha_{zz})^2 + (\alpha_{zz} - \alpha_{xx})^2 + 6\left(\alpha_{xy}^2 + \alpha_{yz}^2 + \alpha_{xz}^2\right)\Big]^{1/2} \tag{6}$$

$$\beta_0 = (\beta_x^2 + \beta_y^2 + \beta_z^2)^{1/2} \tag{7}$$

The total dipole moment (μ), polarizability (α) and first hyperpolarizability (β_0), of (*E*)-2HBAPPA is calculated using B3LYP/6-311++G(d,p) basis set. The electric dipole moment, polarizability and hyperpolarizability of (*E*)-2HBAPPA are shown in Table 3. The total dipole moment (μ = 1.3575 Debye) and the first hyperpolarizability ($\beta_0 = 5.3341 \times 10^{-30}$ esu) of the title molecule is 14 times greater than that of urea, hence this molecule has considerable NLO activity (μ and β of urea are 1.3732 Debye and 0.3728×10^{-30} esu, respectively).

4.4. NBO analysis

The hyperconjugation may be given as stabilizing effect that arises from an overlap between an occupied orbital with another neighboring electron deficient orbital, when these orbitals are properly orientated. This non-covalent bonding-antibonding interaction can be quantitatively described in terms of the NBO analysis, which is expressed by means of the second-order perturbation interaction energy ($E^{(2)}$) [52–55]. This energy represents the estimate of the off-diagonal NBO Fock matrix elements. It can be deduced from the second-order perturbation approach [56].

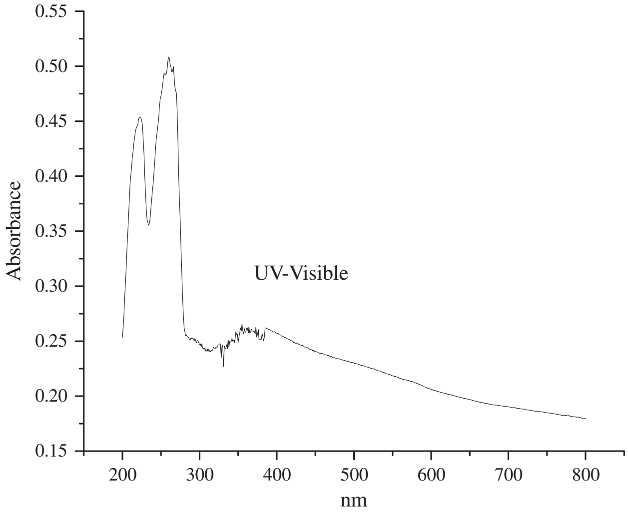

Fig. 5. The UV–Visible spectrum of (*E*)-2HBAPPA.

$$E^{(2)} = \Delta E_{ij} = q_i \frac{F(i,j)^2}{\varepsilon_j - \varepsilon_i} \tag{2}$$

where q_i is the donor orbital occupancy, ε_i and ε_j are diagonal elements (orbital energies) and $F(i,j)$ is the off diagonal NBO Fock matrix elements.

The NBO analysis has been carried out on the molecule using B3LYP/6-311++G(d,p) basis set. The electron densities, $E^{(2)}$ values and types of interaction are listed in Table 4. In this study, the σ bonds have higher electron density than the π bonds. Due to this reason, the σ–σ* transitions have minimum delocalization energy than the π–π* transitions. It is evident from the Table 4 that the $C_1—C_2$ bond transfer energy 9.96 and 8.12 kJ/mol to the acceptor orbital of $C_1—C_6$ and $O_{21}—H_{22}$ respectively. The electron density of $C_1—C_2$ (*i*) and $C_1—C_6$, $O_{21}—H_{22}$ (*j*) are 1.978 and 0.013, 0.073e respectively. There occurs a strong intra-molecular hyperconjugative interaction of π electrons from $C_1—C_6$, $C_4—C_5$, $C_{25}—C_{26}$, $C_{27}—C_{30}$ and $C_{28}—C_{32}$ bonds to the π* $C_4—C_5$, $C_1—C_6$, ($C_{27}—C_{30}$, $C_{28}—C_{32}$), ($C_{25}—C_{26}$, $C_{28}—C_{32}$) and ($C_{25}—C_{26}$, $C_{27}—C_{30}$) bonds, which increase the electron densities 0.313, 0.013, (0.333, 0.332), (0.343, 0.332) and (0.343, 0.333) leading to stabilization of 67.24, 91.67, (84.85, 86.86), (85.06, 82.51) and (84. 10, 87.07) kJ/mol, respectively. The lone pair electrons are readily available for the interaction with excited electrons of acceptor antibonding orbital. During the n → π* transition, more energy delocalization takes place. The LPC_3 (1.109e) transfer the energy 282.46 and 291.16 kJ/mol to antibond

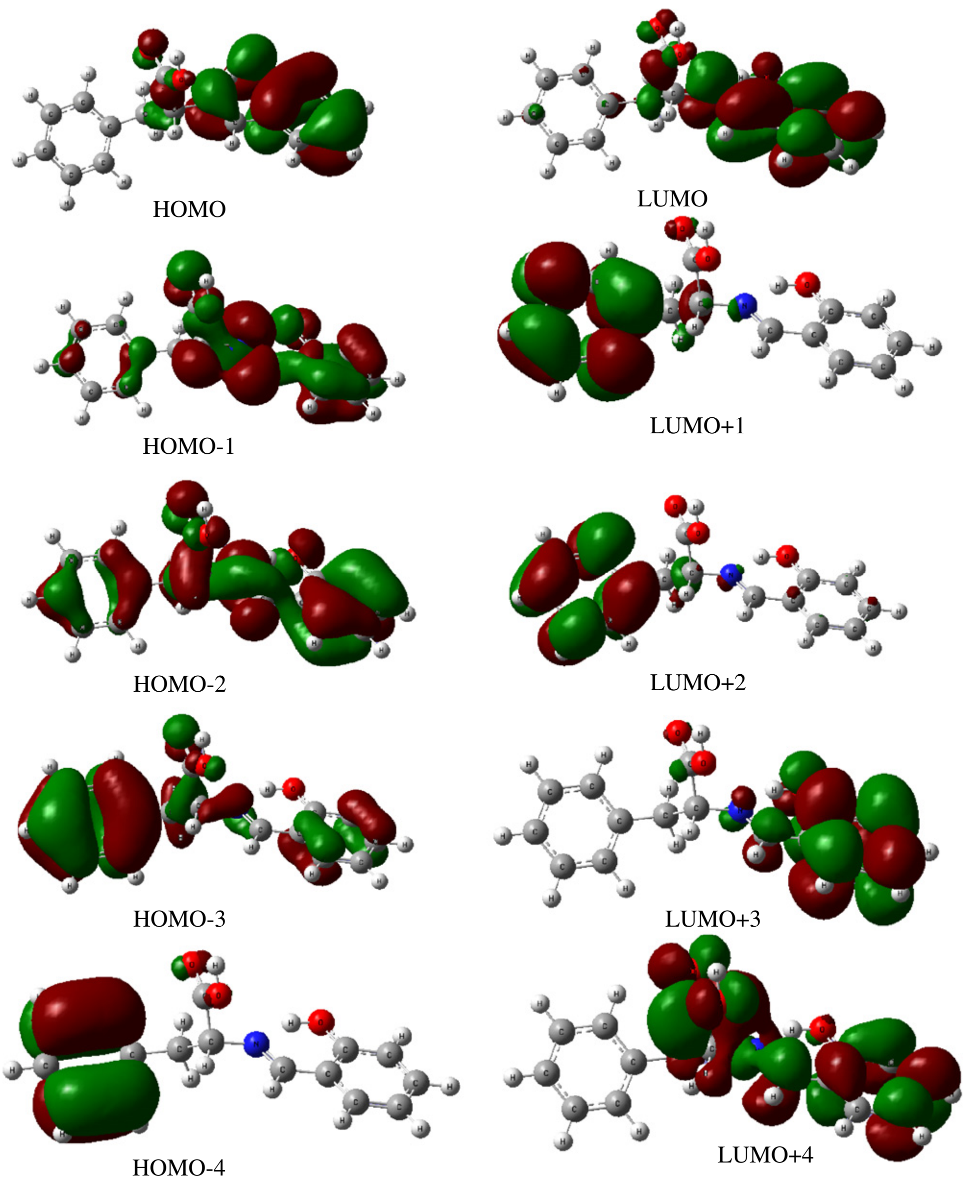

Fig. 6. The frontier molecular orbitals of (*E*)-2HBAPPA.

of $C_4—C_5$ (0.313e) and $C_{11}—N_{23}$ (0.179e) respectively. Similarly the LPO_{19} (1.812e) to its antibonding $C_{17}—O_{18}$ (0.206) is about 202.92 kJ/mol. In this study, the intra-molecular $O_{21}—H_{22}\cdots N_{23}$ hydrogen bond is exposed in the NBO analysis, results shown in Table 4 by the interaction between the nitrogen lone pair and $O_{21}—H_{22}$ antibonding orbital $LPN_3 \rightarrow \pi^*$ $(O_{21}—H_{22})$ with stabilization energy 120 kJ/mol.

4.5. HOMO–LUMO analysis

The electronic absorption and HOMO and LUMO energies were calculated respectively using TD-DFT and DFT methods with 6-311++G(d,p) basis set and are listed in the Table 5. The calculated HOMO–LUMO energy gap is −4.4094 eV and the calculated band gaps are comparable with recorded UV–Vis results. The first excited state (E_1) lies at 68 → 76 ($HOMO_{-3}$–$LUMO_{-4}$) and 71 → 72 (HOMO–LUMO). The band gap of the first state (E_1) is observed at 314.65 nm, whereas the calculated value is 318.91 nm. The $HOMO_{-3}$ is located over the conjugated C—C—C of phenyl ring and LUMO is located over the each atom of phenol ring. It is evident from Table 5, the second excited state observed at 276.32 nm. The calculated value for the same is observed at 276.72 nm, which consist two sub-energy levels namely $HOMO_{-4}$–LUMO (67 → 72) and $HOMO_{-1}$–LUMO (70 → 72). Similarly third excited state lies at 67 → 72 ($HOMO_{-4}$–LUMO) and 69 → 72 ($HOMO_{-2}$–LUMO) and is located over each atom of the molecule. The observed and calculated band gap for the corresponding excited state is 254.11 nm and 264.49 nm. The recorded UV–Vis, spectrum and HOMO–LUMO plots are shown in Figs. 5 and 6, respectively.

5. Conclusion

The molecule (*E*)-2-HBAPPA was synthesized and a complete vibrational analysis has been carried out for the first time. The various possible conformers are evaluated using B3LYP/6-311++G(d,p) basis set and most stable conformer is conformer one. The *ab initio* DFT calculations have been carried out on the structure and vibrational spectrum of (*E*)-2-HBAPPA. Comparison between the calculated and experimental structural parameters indicates that the results of B3LYP/6-311++G(d,p) are in agreement with literature. Vibrational frequencies calculated by B3LYP/6-311++G(d,p) method agree very well with experimental results. The close agreement established between the experimental and scaled frequencies obtained using the large basis set (6-311++G(d,p)) calculation has proved the accuracy of the DFT method of calculations. Optimized geometry indicates intra-molecular ($O_{21}—H_{22}\cdots N_{23}$) hydrogen bonding in the molecule. Vibrational spectra and NBO analysis confirm the occurrence of blue shifting hydrogen bond in the molecule. The calculated first hyperpolarizability is found to be 5.3341×10^{-30} esu, which is 14 times greater than that of urea which imply that the title compound might become a kind of good NLO material. NBO result reflects the charge transfer mainly due to π–π^* transitions in the phenyl and phenol rings. The lowering of HOMO and LUMO energy gap clearly explains the charge transfer interaction taking place within the molecule. A good correlation between the UV–Vis, absorption maxima and calculated electronic absorption maxima are found.

Acknowledgements

One of the authors (Y. Erdogdu) would like to thank Ahi Evran University Research Fund for its financial support, Project Numbers: FBA-11-09. Computing resources used in this work were provided by the National Center for High Performance Computing of Turkey (UYBHM). The corresponding author (H. Saleem) would like to thank Annamalai University (India, Tamilnadu) to provided the “100th Ph.D. (in Physics) awardees endowment” for one of his Ph.D. scholar (S. Subashchandrabose).

Appendix A. Supplementary material

Supplementary data associated with this article can be found, in the online version, at http://dx.doi.org/10.1016/j.molstruc.2012.04.011.

References

[1] D.A. Atwood, M.J. Harvey, Chem. Rev. 101 (2001) 37–52.
[2] N. Hoshino, Coord. Chem. Rev. 174 (1998) 77–108.
[3] Y. Wang, J.L. DuBois, B. Hedman, K.O. Hodgson, Stack TDP Sci. 279 (1998) 537–540.
[4] P.A. Vigato, S. Tamnurini, Coord. Chem. Rev. 248 (2004) 1717–2128.
[5] H. Karabiyik, H. Petek, N.O. Iskeleli, C. Albayrak, Struct. Chem. 20 (2009) 1055–1065.
[6] H. Petek, C. Albayrak, M. Odabosoglu, I. Senel, O. Buyukgungor, Struct. Chem. 21 (2010) 681–690.
[7] T. Sekikawa, T. Kobayashi, T. Inabe, J. Phys. Chem. A101 (1997) 644–649.
[8] J. Rhodes, H. Chen, S.R. Hall, J.E. Beesley, D.C. Jenkins, P. Collins, B. Zheng, Nature 377 (1995) 71.
[9] B. Zheng, S. Brett, J.P. Tite, T.A. Brodie, J. Rhodes, Science 256 (1992) 1560.
[10] P.C.J. Doubell, D.W. Oliver, Arzeim-Forsch./Drug Res. 42 (1992) 65.
[11] E.J. Lien, in: E. Jucker (Ed.), Progress in Drug Research, 40 Birkhauser, Basel, 1993, pp. 163–189.
[12] T. Maekawa, S. Vamamoto, Y. Igata, S. Ikeda, T. Watanabe, M. Shiraishi, Chem. Pharm. Bull. 45 (1997) 1994–2004.
[13] Y.Z. Xiong, F.E. Chen, J. Balzarini, E.D. Clercq, C. Pannecouque, Eur. J. Med. Chem. 43 (2008) 1230–1236.
[14] D. Sriram, P. Yogeeswari, N. Sirisha, V. Saraswat, Bioorg. Med. Chem. Lett. 16 (2006) 2127–2129.
[15] H. Zhao, N. Neamati, S. Sunder, H. Hong, S. Wang, G.W.A. Milne, Y. Pommier, T.R. Burke, J. Med. Chem. 40 (1997) 937–941.
[16] G. Liu, J. Peiliao, S. Huang, G. Lishen, R. Qinyu, Anal. Sci. 17 (2001) 1031–1035.
[17] P.H. Wang, J.G. Keck, E.J. Lien, M.M.C. Lai, J. Med. Chem. 33 (1990) 608–614.
[18] V.I. Prisakar, V.I. Tsapkov, S.A. Buracheéva, M.S. Byrké, A.P. Gulya, J. Pharm. Chem. 39 (2005) 313–315.
[19] L. Lazzarato, M. Donnola, B. Rolando, E. Marini, C. Cena, G. Coruzzi, E. Guaita, G. Morini, R. Fruttero, A. Gasco, S. Biondi, E. Ongini, J. Med. Chem. 51 (2008) 1894–1903.
[20] E.S. Howard, E.P. Burrows, M.J. Marks, R.D. Lynch, Fu-Mingchen, J. Am. Chem. Soc. 99 (1977) 707–713.
[21] M.J. Frisch, G.W. Trucks, H.B. Schlegel, G.E. Scuseria, M.A. Robb, J.R. Cheeseman, J.A. Montgomery Jr., T. Vreven, K.N. Kudin, J.C. Burant, J.M. Millam, S.S. Iyengar, J. Tomasi, V. Barone, B. Mennucci, M. Cossi, G. Scalmani, N. Rega, G.A. Petersson, H. Nakatsuji, M. Hada, M. Ehara, K. Toyota, R. Fukuda, J. Hasegawa, M. Ishida, T. Nakajima, Y. Honda, O. Kitao, H. Nakai, M. Klene, X. Li, J.E. Knox, H.P. Hratchian, J.B. Cross, C. Adamo, J. Jaramillo, R. Gomperts, R.E. Stratmann, O. Yazyev, A.J. Austin, R. Cammi, C. Pomelli, J.W. Ochterski, P.Y. Ayala, K. Morokuma, G.A. Voth, P. Salvador, J.J. Dannenberg, V.G. Zakrzewski, S. Dapprich, A.D. Daniels, M.C. Strain, O. Farkas, D.K. Malick, A.D. Rabuck, K. Raghavachari, J.B. Foresman, J.V. Ortiz, Q. Cui, G. Baboul, S. Clifford, J. Cioslowski, B.B. Stefanov, G. Liu, A. Liashenko, P. Piskorz, Komaromi, R.L. Martin, D.J. Fox, T. Keith, M.A. Al-Laham, C.Y. Peng, A. Nanayakkara, M. Challacombe, P.M.W. Gill, B. Johnson, W. Chen, M.W. Wong, C. Gonzalez, J.A. Pople, Gaussian 03, Revision C.02, Gaussian, Inc., Wallingford, CT, 2004.
[22] H.B. Schlegel, J. Comput. Chem. 3 (1982) 214–218.
[23] Spartan 08, Wavefunction Inc., Irvine, CA 92612, USA, 2008.
[24] G. Rauhut, P. Pulay, J. Phys. Chem. 99 (1995) 3093.
[25] D. Michalska, Raint Program, Wroclaw University of Technology, 2003.
[26] D. Michalska, R. Wysokinski, Chem. Phys. Lett. 403 (2005) 211–217.
[27] A.D. Khalaji, A.N. Chermahini, K. Fejfarova, M. Dusek, Struct. Chem. 21 (2010) 153–157.
[28] Y. Wang, Z. Yu, Y. Sun, Y. Wang, L. Lu, Spectrochim. Acta A 79 (2011) 1475–1482.
[29] A.R. Choudhury, T.N. Guru Row, Acta Crystallogr. E60 (2004) o1595–o1597.
[30] D. Sajan, Y. Erdogdu, T. Kuruvilla, I. Hubert Joe, J. Mol. Struct. 983 (2010) 12–21.
[31] M. Jadrijevic, M. Takać, D.V. Topić, Acta Pharm. 54 (2004) 177.
[32] C. Meganathan, S. Sabastian, M. Kurt, K. Woolee, N. Sundaraganesan, J. Raman Spectrosc. 42 (2010) 1369–1378.
[33] V. Krishnakumar, R. Mathammal, J. Raman Spectrosc. 40 (2009) 264.
[34] N. Sundaraganesan, B.D. Joshua, K. Settu, Spectrochim. Acta A 66 (2007) 381.
[35] M. Selverstein, G.C. Basseler, C. Morill, Spectrometric Identification of Organic Compounds, Wiley, New York, 1981.
[36] Y. Akkaya, S. Akyűz, Vib. Spectrsoc. 42 (2006) 292.
[37] S. Subashchandrabose, H. Saleem, Y. Erdogdu, O. Dereli, V. Thanikachalam, J. Jayabharathi, Spectrochim. Acta A 86 (2012) 231–241.
[38] W. Kemp, Organic Spectroscopy, third ed., W.H. Freeman & Co, 1991.
[39] G. Litiuinov, in: Proceedings of the 13th International Conference on Raman Spectroscopy, Wurznyrg, Germany, 1992.
[40] K. Furic, V. Mohacck, M. Bonifacic, I. Stefanic, J. Mol. Struct. 267 (1992) 39.
[41] G. Lsu, H. Wang, Spectrochim. Acta 46A (1990) 1211.
[42] J.G. Mesu, T. Visser, F. Soulimani, B.M. Weckhuysen, Vib. Spectrosc. 39 (2005) 114.
[43] Y. Hung, D.F.R. Gilso, I.S. Butlei, J. Chem. Phys. 97 (1993) 1998.
[44] D.N. Sathyanarayanan, Vibrational Spectroscopy – Theory and Applications, second ed., New Age international (P) Limited Publisher, New Delhi, 2004.
[45] M.K. Subramanian, P.M. Anbarasan, S. Manimegali, J. Raman Spectrosc. 40 (2009) 1657–1663.
[46] H.T. Varghesa, C.Y. Paniker, V.S. Madhavan, S. Mathew, J. Vinsova, C.V. Alsenoy, J. Raman Spectrosc. 40 (2009) 1211–1223.
[47] A. Filarowski, A. Koll, A. Karpfen, P. Wolschann, Chem. Phys. 297 (2004) 323–332.
[48] J. Pajak, G. Maes, W.M. De Borggraeve, N. Boens, A. Filarowski, J. Mol. Struct. 844–845 (2007) 83–93.
[49] V. Krishnakumar, K. Murugeswari, N. Prabavathi, R. Mathammal, Spectrochim. Acta A 91 (2012) 1–10.
[50] L.J. Belemy, The Infrared Spectra of Complex Molecule, third ed., Wiley, New York, 1975.
[51] N.B. Colthup, L.H. Daly, S.E. Wiberly, Introduction to Infrared and Raman Spectroscopy, Academic Press, New York, 1990.
[52] A.E. Reed, F. Weinhold, J. Chem. Phys. 83 (1985) 1736.
[53] A.E. Reed, R.B. Weinstock, F. Weinhold, J. Chem. Phys. 83 (1985) 735.
[54] A.E. Reed, F. Weinhold, J. Chem. Phys. 78 (1983) 4066.
[55] J.P. Foster, F. Wienhold, J. Am. Chem. Soc. 102 (1980) 7211–7218.
[56] J. Chocholousova, V. Vladimir Spirko, P. Hobza, Phys. Chem. Chem. Phys. 6 (2004) 37–41.